© 2017. Published by The Company of Biologists Ltd | Development (2017) 144, 281-291 doi:10.1242/dev.141259

RESEARCH ARTICLE

Basal filopodia and vascular mechanical stress organize fibronectin into pillars bridging the mesoderm-endoderm gap

Yuki Sato[1,2,*], Kei Nagatoshi[1], Ayumi Hamano[3], Yuko Imamura[4], David Huss[5,6], Seiichi Uchida[3] and Rusty Lansford[5,6]

ABSTRACT

Cells may exchange information with other cells and tissues by exerting forces on the extracellular matrix (ECM). Fibronectin (FN) is an important ECM component that forms fibrils through cell contacts and creates directionally biased geometry. Here, we demonstrate that FN is deposited as pillars between widely separated germ layers, namely the somitic mesoderm and the endoderm, in quail embryos. Alongside the FN pillars, long filopodia protrude from the basal surfaces of somite epithelial cells. Loss-of-function of Ena/VASP, α5β1-integrins or talin in the somitic cells abolished the FN pillars, indicating that FN pillar formation is dependent on the basal filopodia through these molecules. The basal filopodia and FN pillars are also necessary for proper somite morphogenesis. We identified a new mechanism contributing to FN pillar formation by focusing on cyclic expansion of adjacent dorsal aorta. Maintenance of the directional alignment of the FN pillars depends on pulsatile blood flow through the dorsal aortae. These results suggest that the FN pillars are specifically established through filopodia-mediated and pulsating force-related mechanisms.

KEY WORDS: Fibronectin, Filopodia, Somite, Endoderm, Dorsal aorta

INTRODUCTION

Three-dimensional (3D) organization of the extracellular matrix (ECM) is crucial for configuring tissue and organ shape and function (Rozario and DeSimone, 2010). Understanding how the ECM is patterned and how cells sense and react to ECM patterning are key to understanding the cellular and molecular mechanisms driving tissue morphogenesis. Several studies have shown that physical properties of the ECM, including geometry, rigidity and tension, may influence the forces exerted on cells, which in turn affect cell shape and ultimately lead to the modification of fundamental cellular processes such as migration and differentiation *in vitro* (DuFort et al., 2011). However, with regard to dynamic morphogenesis during embryo development, the interplay between cell cytoskeletal architecture and ECM properties and related tensional forces is poorly understood.

Fibronectin (FN) is an ECM component that is essential for the morphogenesis of various tissues and organs (Rozario and DeSimone, 2010). The generation of FN fibrils is connected to dynamic cell rearrangement events during tissue morphogenesis (Jülich et al., 2015; Dzamba et al., 2009; Martins et al., 2009). For example, binding of FN to α5β1-integrins and their associated cytoplasmic adaptor proteins (talin, vinculin) promotes FN polymerization into fibrils. In addition, intrinsic and/or extrinsic mechanical forces can promote FN fibrillogenesis and fibril alignment to the direction of force (Baneyx et al., 2001, 2002; Little et al., 2008; Hytönen and Wehrle-Haller, 2016). Given that FN fibers can stretch 5- to 6-fold *in vitro* (Little et al., 2008; Smith et al., 2007), it is enticing to speculate that they could be involved in matrix elasticity between separated tissues.

In early amniote embryos, the somitic mesoderm and endoderm are separated by a 40-50 µm gap. The paired dorsal aortae arise and migrate through this space (Sato, 2013). Here, we report that the gap between somitic mesoderm and endoderm is spanned by pillar-like arrangements of FN fibrils, together with long filopodia emanating from the basal surfaces of somitic epithelial cells. We discovered these FN pillars by studying FN distribution in a transgenic quail embryo model system, using tissue-specific DNA electroporation and time-lapse imaging (Bower et al., 2011). The PGK:H2B-mCherry transgenic quail embryo enables us to track every cell and ECM dynamics over time in living embryos, and to study cell-autonomous roles of electroporated genes (Huss et al., 2015). This approach allowed us to visualize the previously unknown pattern of FN in the somite-endoderm gap. In striking contrast to previously reported patterns of FN distribution near the basal surfaces of cells, we found that the FN pillars extend far away from cell bodies into the gap space. The directional arrangement of the FN pillars and their accompanying somite cell filopodia suggested that they might be patterned by a site-specific tensional force. Subsequent experiments suggest that cyclic tensional forces associated with pulsation of the dorsal aortae are involved in formation of the FN pillars.

RESULTS

FN forms pillars between somites and endoderm

Using confocal laser microscopy of whole-mount immunostained quail embryos at the early somitogenesis stage and subsequent reconstruction of optical sections, we observed many long FN fibrils patterned as pillars (~40-50 µm in length) in the gap between somites and endoderm tissues (lower panels in Fig. 1B,C). FN around the somite epithelium is known to be required for somite boundary formation and cell rearrangement during somite epithelialization in various vertebrate embryos (Girós et al., 2011; Jülich et al., 2015; Koshida et al., 2005; Martins et al., 2009; Rifes

[1]Department of Anatomy and Cell Biology, Graduate School of Medical Sciences, Kyushu University, 3-1-1 Maidashi, Higashi-ku, Fukuoka 812-8582, Japan. [2]JST, PRESTO, 4-1-8 Honcho, Kawaguchi, Saitama 332-0012, Japan. [3]Department of Advanced Information Technology, Faculty of Information Science and Electrical Engineering, Kyushu University, 744 Motooka, Nishi-ku, Fukuoka 819-0385, Japan. [4]Graduate School of Science, Kumamoto University, 2-39-1 Kurokami, Chuo-ku, Kumamoto 860-8555, Japan. [5]Department of Radiology and Developmental Neuroscience Program, Saban Research Institute, Children's Hospital Los Angeles, Los Angeles, CA 90027, USA. [6]Department of Radiology, Keck School of Medicine, University of Southern California, Los Angeles, CA 90089, USA.

*Author for correspondence (satoyuki@anat1.med.kyushu-u.ac.jp)

Y.S., 0000-0001-8974-2059; A.H., 0000-0002-7115-0626; S.U., 0000-0001-8592-7566; R.L., 0000-0002-2159-3699

Received 17 June 2016; Accepted 29 November 2016

Development (2017) 144, 281-291 doi:10.1242/dev.141259

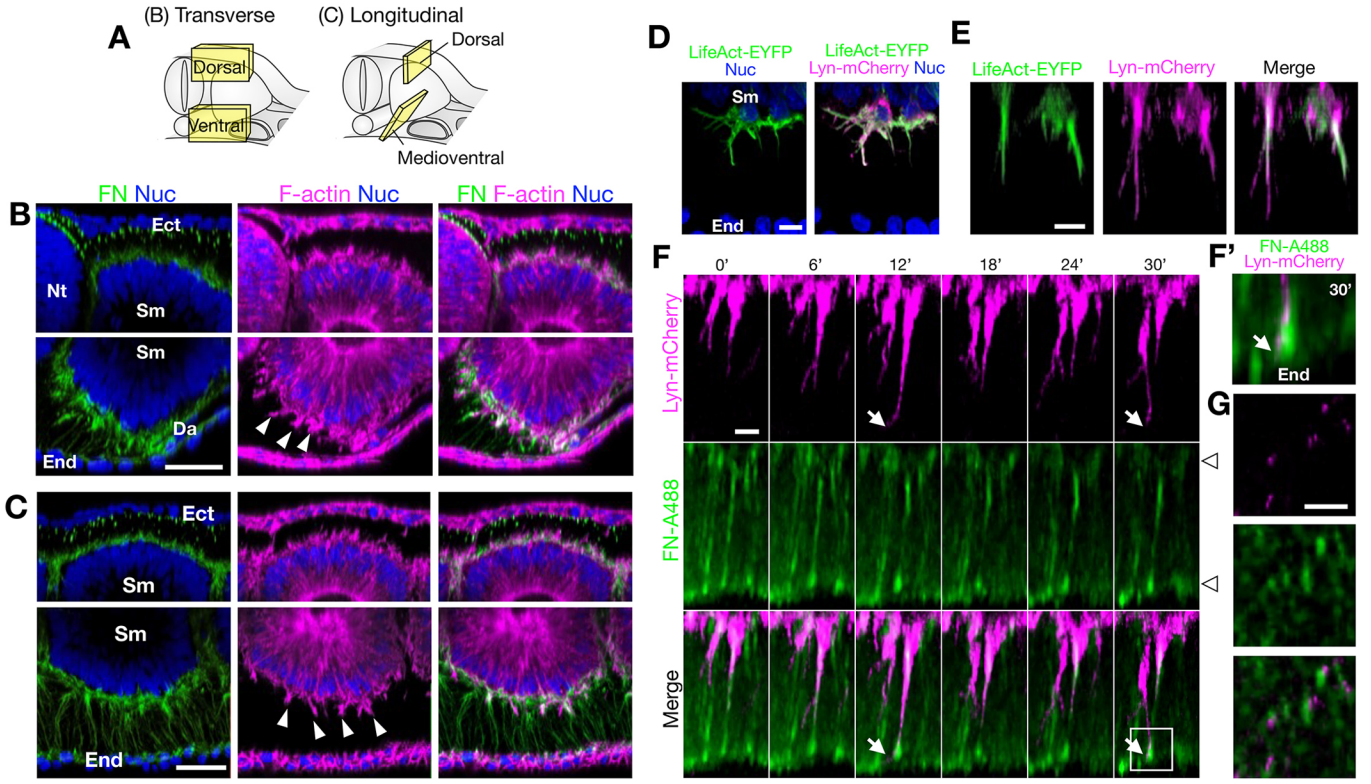

Fig. 1. The FN and filopodia distribution between somites and endoderm resembles architectural pillars. (A-C) Optically reconstructed transverse (B) and longitudinally oblique (C) sections at the SIV somite level of a representative HH stage 12 quail embryo. Positions of the sections are indicated in A. Staging of the somites is described by Ordahl (1993). FN is detected by anti-FN immunostaining. F-actin and nuclei were detected by phalloidin and Hoechst, respectively. Upper and lower panels show the dorsal and ventral parts of a somite, respectively. FN was distributed as granules beneath the ectoderm (upper panels) and as short fibrils dorsal to the somite (lower panels). F-actin-accumulated longer spikes were observed in the medioventral surface of somite (arrowheads). (D,E) F-actin and cell membranes of somitic epithelial cells were labeled with LifeAct-EYFP and Lyn-mCherry, respectively, following electroporation. Each panel shows a longitudinally oblique section at the SIV level in HH stage 12 embryos. EYFP lines mCherry in every filopodium protruding from somite epithelial cells in a fixed embryo (D). Stills from time-lapse imaging of LifeAct-EYFP- and Lyn-mCherry-labeled filopodia (E, see also Movie 1). (F) Time-lapse imaging of FN-Alexa488 and Lyn-mCherry-labeled filopodia at the SIV level in a HH stage 12 embryo. Each panel shows longitudinal oblique sections at 6 min intervals (see also Movie 2). Lyn-mCherry-labeled filopodia repeat elongation/retraction along the FN pillars and reach the endoderm (arrows; boxed region is enlarged in F′). Proximal FN layers of somites and endoderm are indicated by open arrowheads (alongside middle panels). (G) A cross-section of vitally imaged filopodia and FN pillars. Lyn-mCherry and FN-Alexa488 signals are adjacent to each other. Somite cells were partially labeled by electroporation; thus, fewer Lyn-mCherry signals were observed than FN-Alexa488 signals. Anterior is left in C-G. Ect, ectoderm; Sm, somite; Nt, neural tube; End, endoderm; Da, dorsal aorta. Scale bars: 40 µm in B,C; 10 µm in D-G.

et al., 2007). Fibrillar FN spanning the somite-endoderm gap has been imaged in chicken embryos using a similar approach (Rifes and Thorsteinsdóttir, 2012). However, the mechanism underlying the construction of these long, thick FN pillars between somites and endoderm has not been studied. The FN pillars in the somite-endoderm gap were observed at early stages of somite differentiation and throughout epithelial somites (prior to delamination, lower panels in S0, IV, VI in Fig. S1B,D). Using the F-actin marker phalloidin, we also found elongated protrusions extending from the basal surfaces of the somitic epithelial cells (arrowheads in Fig. 1B,C). Since these protrusions contained F-actin, we designated them as filopodia.

To dynamically observe the filopodia in more detail, cell membranes and F-actin were fluorescently labeled with Lyn-mCherry and LifeAct-EYFP (Abe et al., 2011; Riedl et al., 2008), respectively, by somite-specific electroporation (Fig. S2). In fixed embryos, multiple filopodia protruded from the basal surfaces of somitic epithelial cells and F-actin lined every filopodia membrane (n=6, Fig. 1D). To assess the possibility of fixation-induced changes in the somitic cell filopodia, we studied filopodial dynamics in living embryos by time-lapse imaging. The mCherry-labeled cell membrane profiles and EYFP-labeled F-actin profiles of the filopodia were longer than those seen in the fixed embryos, indicating that fixation shrinks the filopodia (n=4, Fig. 1E, Movie 1).

To further confirm the spatial relationship between the FN pillars and filopodia, we exploited the polymerization property of FN for vital labeling of the pillars (Hoffmann et al., 2008). Alexa 488-conjugated FN (FN-Alexa488) solution was injected into the Lyn-mCherry-electroporated embryos, and the embryos were then imaged by confocal laser microscopy. The FN-Alexa488 was distributed within the pillar-like structures and repetitive protrusion/regression of mCherry-positive filopodia was observed (n=5, Fig. 1F, Movie 2). Optical cross-sections at the mid-level of the somite-endoderm gap showed that filopodia and FN pillars lay in close proximity (Fig. 1G). Importantly, time-lapse imaging analysis revealed that the filopodia were elongated and oriented along the FN pillars. At points where the filopodia were maximally elongated they transiently reached the endoderm (arrows in Fig. 1F,F′).

FN pillars and basal filopodia are mutually dependent

Ena/VASP proteins recruit the F-actin cytoskeleton to membrane-anchored adaptor proteins at the tip of the filopodium, where they

Development (2017) 144, 281-291 doi:10.1242/dev.141259

promote actin filament elongation and are required for filopodial formation (Bear and Gertler, 2009). We found that both *Ena* and *VASP* mRNAs were expressed in the somites (Fig. S3). In addition, when EYFP-tagged Ena and VASP proteins were expressed in the somites, the proteins were localized to the filopodia of somite epithelial cells (Fig. S4). These results suggest the involvement of Ena/VASP in filopodia formation in the somites. To further examine the relationship between the somitic epithelial basal filopodia and the FN pillars, we disrupted filopodia formation by perturbing Ena/VASP subcellular localization. Ena/VASP can be depleted from the filopodia and mislocalized onto the mitochondrial surface by overexpressing FPPPP (FP4)-mito through four EVH1 binding sites (Bear et al., 2000). We confirmed that overexpression of FP4-mito depleted Ena/VASP in quail embryonic fibroblasts (Fig. S5).

The somitic filopodia and FN pillars remained intact after the embryos were co-electroporated with a control construct APPPP (AP4)-mito that does not bind Ena/VASP proteins (Bear et al., 2000) and Lyn-mCherry, and upon injection of FN-Alexa488 (n=5, Fig. 2A, Movie 3). By contrast, when FP4-mito was co-expressed with Lyn-mCherry in somitic cells, FN pillars were not observed where filopodia protrusion was disturbed (n=8, Fig. 2B, Movie 4). Sparse FN pillars were found underneath the FP4-mito-overexpressing somites, as non-electroporated cells were present in a patchy distribution. To quantitatively evaluate the effect of FP4-mito overexpression on FN pillar formation, we measured the number of FN pillars. The average number of FN pillars was reduced in the somite-endoderm gaps beneath FP4-mito-electroporated somites (Fig. 2C,D). Quantitative RT-PCR (qRT-PCR) analysis of SI to VIII level somites isolated from electroporated embryos confirmed that quail fibronectin 1 (*FN1*) mRNA levels were comparable between AP4-mito-electroporated and FP4-mito-electroporated somites, indicating that loss of the filopodia does not affect FN expression levels (Fig. 2E). Thus, the basal filopodia appear to be required specifically for the formation of the FN pillars.

The requirement of the FN pillars for filopodial elongation was next tested by expressing a 70 kDa N-terminal fragment of FN that inhibits polymerization of endogenous FN fibrils when strongly expressed (Martins et al., 2009). Twenty-four hours after electroporation of the 70 kDa N-terminal fragment of quail FN1 (70 kDa qFN) into somite precursors and nascent endoderm, we observed ectopic, granular FN in the somite-endoderm gap, and filopodia were not elongated (lower panels in Fig. 2F). This suggests that polymerization of FN is required for both formation of the FN pillars and for basal filopodia elongation.

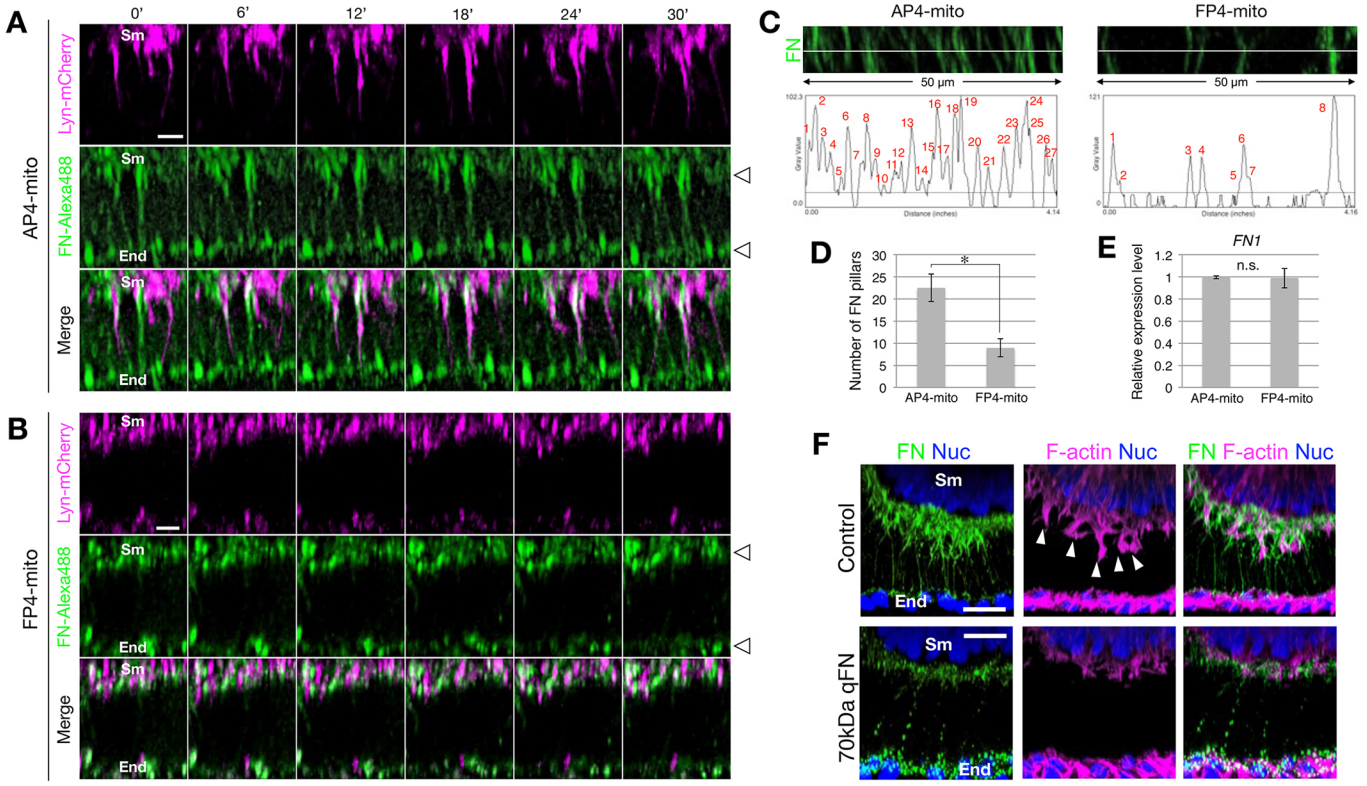

Fig. 2. Defects in filopodia induced by Ena/VASP depletion reduce FN pillars. (A,B) Time-lapse imaging of FN and filopodia in a control (A) and an Ena/VASP-depleted (B) embryo. FN and filopodia were visualized by FN-Alexa488 and Lyn-mCherry. Each panel shows a time series of longitudinal oblique sections of the medioventral side of a somite at SIV level in a HH stage 12 embryo at 6 min intervals. (A) AP4-mito-overexpressing somite cells (control) protrude mCherry-positive filopodia toward the endoderm along the FN pillars (see also Movie 3). (B) FP4-mito-overexpressing somite cells do not protrude filopodia and FN pillars are not observed (see also Movie 4). The distribution of proximal FN to the somites and endoderm is not affected (open arrowheads). (C) Cropped images (50 μm width) at the middle levels of the somite and endoderm gap in AP4-mito- and FP4-mito-overexpressing embryos (upper panels). The number of FN pillars crossing the horizontal line was counted using the ImageJ plot profile program (lower panels). (D) The number of FN pillars crossing the 50 μm horizontal line was reduced in FP4-mito-electroporated embryos. Averages of seven independent embryos are shown. *P<0.0001 by Student's t-test. Error bars represent s.d. (E) *FN1* expression levels in EGFP-AP4-mito- and EGFP-FP4-mito-electroporated somites as quantified by qRT-PCR. The sample collection procedure is indicated in Fig. 7A. FP4-mito overexpression does not alter the *FN1* expression level in the somites. Error bars represent s.d. (F) Inhibition of FN assembly by overexpression of 70 kDa qFN. Electroporation with an empty expression vector did not alter FN pillars and F-actin spikes (n=10; arrowheads). In 70 kDa qFN-electroporated embryos, granular FN appeared ectopically and F-actin spikes were not elongated (n=14; lower panels). Anterior is left. Scale bars: 10 μm in A,B; 20 μm in F. Sm, somite; End, endoderm.

Development (2017) 144, 281-291 doi:10.1242/dev.141259

Somite and endoderm provide FN to their gap space

The expression pattern of endogenous quail *FN1* mRNA indicates that a number of heterogeneous tissues produce FN, including the somites and endoderm (Fig. 3A) (Gomes de Almeida et al., 2016). We assessed the contributions of somites and endoderm to the FN pillars by electroporating EGFP-fused quail FN1 (qFN-EGFP) into somitic or endodermal cells. Both electroporated single somitic cells and single endoderm cells were found to provide qFN-EGFP to the pillars (arrowheads in Fig. 3B,C). Because qFN-EGFP electroporation was performed at earlier stages of embryogenesis (Fig. S2), whether qFN-EGFP secretion by somitic mesoderm occurred at the presomitic mesoderm stage or the somite stage remains to be determined. However, these results suggested that both somitic mesoderm and endoderm can provide FN to the FN pillars.

To confirm that both somites and the endoderm contribute to FN pillar formation, we performed tissue-specific shRNA inactivation of endogenous *FN1* mRNA. When *FN1* was inactivated in either somitic or endodermal cells, FN pillars were depleted at positions near the knockdown cells (asterisks in Fig. 3E), and quantitative analysis confirmed that the average number of FN pillars was reduced in these embryos (Fig. 3F). Therefore, both somites and endoderm provide FN to the pillars. Similarly, the reduction of the FN pillars by expression of 70 kDa qFN protein or inactivation of *FN1* mRNA via shRNA electroporation both impaired somite morphogenesis and led to enlargement of somite-endoderm gap spaces (Fig. S6).

β1-containing integrin and talin are required for FN pillar formation

It is known that α5β1-integrin is the primary receptor mediating the assembly of FN (Moser et al., 2009; Shattil et al., 2010), and that the cytoplasmic tail of integrin β1 interacts with the actin cytoskeleton via talin (Jiang et al., 2003; Zhang et al., 2008). We confirmed that integrin β1 and talin are localized within the filopodia of somitic epithelial cells in quail embryos by immunostaining (Fig. 4A,B). To determine if integrin β1 is involved in FN pillar formation, we inactivated integrin β1 mRNA by electroporation of a targeted shRNA vector. We also electroporated the somites with a dominant-negative form of quail talin 1 (qTalin1H) (Zhang et al., 2008). FN pillars did not form beneath integrin β1 knockdown cells (n=18, asterisks in Fig. 4D) or qTalin1H-expressing cells (n=14, asterisks in Fig. 4E) in the somites. As for AP4-mito and FP4-mito overexpression (Fig. 2C), we measured the number of FN pillars in integrin β1 shRNA- and qTalin1H-electroporated embryos. Average numbers of FN pillars were significantly reduced in the somite-endoderm gaps of these embryos (Fig. 4F). Therefore, the distribution of FN pillars appears to depend on both a β1-containing integrin and on talin.

Pillar-like FN distribution is associated with dorsal aorta pulsing

Internal and/or external mechanical forces can unfold FN, exposing internal binding sites that facilitate FN polymerization and subsequent FN fibrillogenesis (Baneyx et al., 2001, 2002; Little

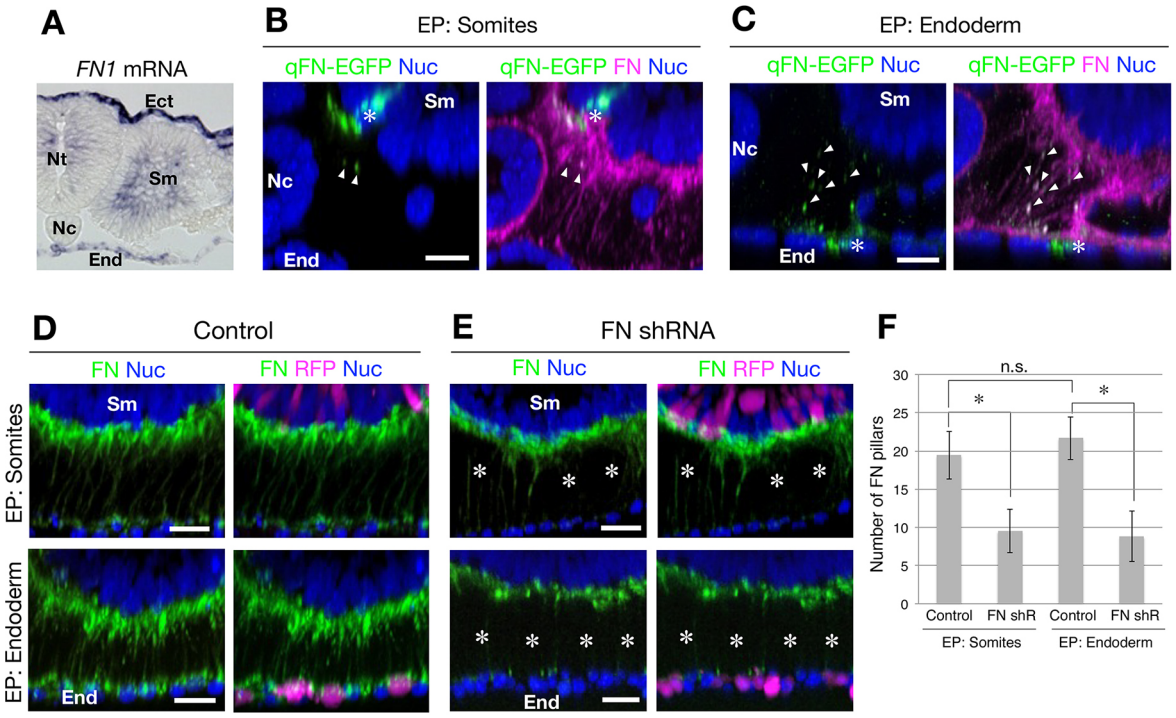

Fig. 3. Both somites and endoderm provide FN to the pillars. (A) *FN1* mRNA expression in a transverse section at the SIV level in a HH stage 12 embryo. *FN1* was expressed in ectoderm, somite, endoderm and neural tube. (B,C) Tracking of somite- or endoderm-derived FN at 24 h after pCAGGSqFN-EGFP electroporation into the somites (B) and endoderm (C, see also Fig. S2). Optical transverse sections at the SIV level in HH stage 12-13 embryos. Endogenous and exogenous FN distribution was detected by anti-FN and anti-GFP immunostaining. Electroporated cells are marked with an asterisk. FN-EGFP signals were found in FN pillars (arrowheads). (D,E) Somite- or endoderm-specific knockdown of FN1. Longitudinal oblique sections at the SIV level in HH stage 12 embryos. Anterior is left. Electroporated cells were detected using RFP (Das et al., 2006). (D) Electroporation of the control vector pRFP-RNAic into either somites or endoderm did not affect FN pillar distribution. (E) Electroporation of pRFP-RNAic-qFN1 reduced FN pillars at positions corresponding to the RFP signals in the somites (asterisks in upper panels) and endoderm (asterisks in lower panels). (F) The number of FN pillars was reduced in both somite- and endoderm-specific expression of *FN1* shRNA. Averages of six independent embryos are shown. *P<0.001 by Student's t-test. Error bars represent s.d. Sm, somite; End, endoderm; Nc, notochord; Nt, neural tube. Scale bars: 20 µm.

Development (2017) 144, 281-291 doi:10.1242/dev.141259

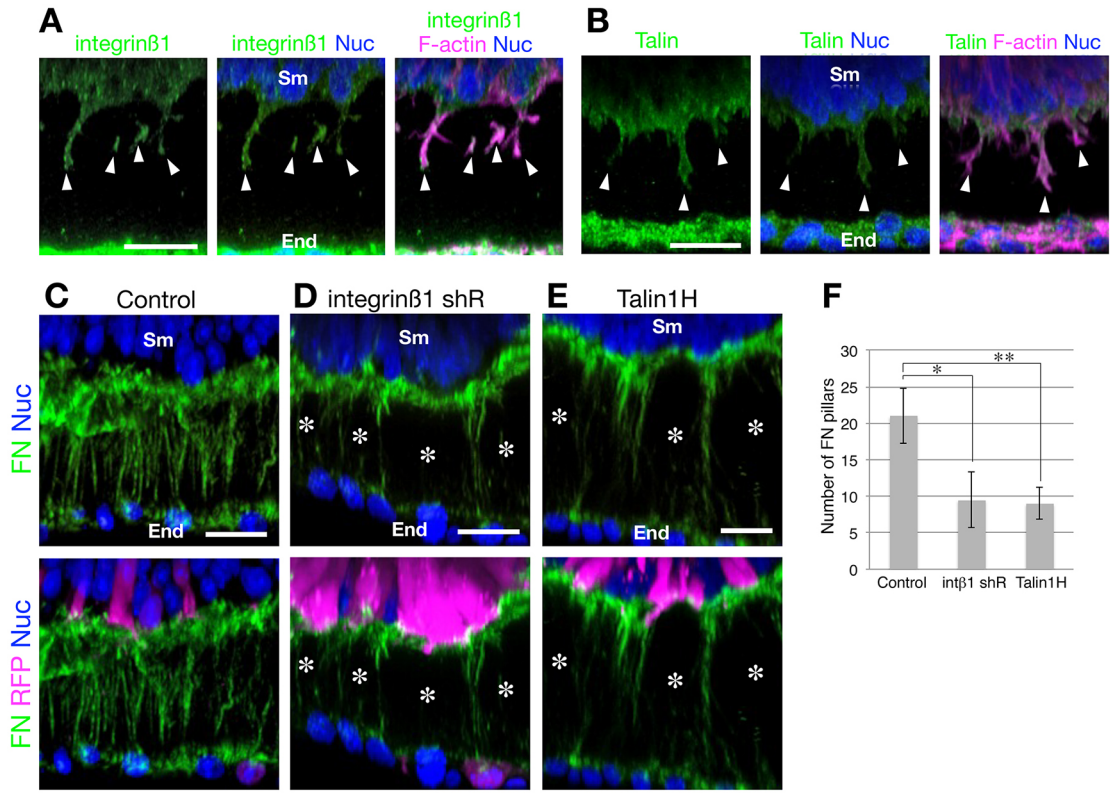

Fig. 4. β1-containing integrin and talin are involved in FN pillar formation. (A,B) Integrin β1 (A) and talin (B) are distributed in the filopodia, as marked with F-actin (arrowheads). (C-E) Loss-of-function experiments for integrin β1 and talin. Electroporated cells were detected by RFP signals. FN pillars were distributed normally in a control embryo (C). FN pillars were absent underneath integrin β1 shRNA-expressing cells (asterisks in D) and qTalin1H-electroporated cells (asterisks in E). (F) The number of FN pillars was reduced in integrin β1 shRNA- and qTalin1H-electroporated embryos. Average values of six independent embryos are given. *P<0.001, **P<0.0001 by Student's t-test. Error bars represent s.d. Each panel shows a longitudinal oblique section of the ventral part of the somites at SIV levels in HH stage 12 embryos. Anterior is left. Sm, somite; End, endoderm. Scale bars: 20 µm.

et al., 2008; Zhong et al., 1998). We therefore investigated the nature and source of the forces inducing fibrillogenesis in the somite-endoderm gap. We hypothesized that the nascent dorsal aorta, which assembles just lateral to FN pillars between the somites and endoderm, might contribute to patterning the pillars. The dorsal aorta walls cyclically expand and contract in response to pulsations in blood flow generated by the beating heart (Movie 5). To test this hypothesis, we disrupted dorsal aorta formation by inhibiting VEGF signaling by Ki8751 treatment, which impedes the differentiation, proliferation and migration of endothelial cells (ECs) (Argraves et al., 2002). We administered Ki8751 at HH stage 10, when the dorsal aortae grow in length and circumference via EC proliferation and migration. The heart kept beating until fixation at HH stage 12 (Movie 6). ECs were detected with the quail EC surface marker QH1 (Pardanaud et al., 1987). The dorsal aortae formed normally in all control embryos (n=7, Fig. 5A), but in all the Ki8751-treated embryos the dorsal aortae appeared abnormal due to disorganized ECs (n=5, upper panels in Fig. 5B). In the Ki8751-treated embryos, EC clusters were found between somites and endoderm, but there were no luminal cavities in these clusters (arrows, lower panel in Fig. 5B). Because functional dorsal aortae were not formed in these embryos, no blood flowed through the embryo body (Movie 6). In control DMSO-administrated embryos, FN was distributed as pillars spanning the somite-endoderm gap, just as it was in unmanipulated control embryos (left panels in Fig. 5D). In the Ki8751-treated, dorsal aorta-deficient embryos, scattering of FN fibril distribution was observed (middle panels in Fig. 5D). Specifically, the vertically aligned distribution of FN fibrils seen in control embryos was disturbed (Fig. 5F) and the length of the FN fibrils was shorter (Fig. 5G). These results support our hypothesis that the dorsal aortae are involved in FN pillar formation within the somite-endoderm gap.

We further examined whether cyclical pulsations of the dorsal aortae caused by the beating heart are involved in establishing the FN pillars. Heart contraction in the quail embryo can be inhibited by the administration of Nifedipine (Bkaily et al., 2003), which blocks L-type Ca^{2+} channels of the myocardium (Navedo and Santana, 2013). The effect of Nifedipine is limited to the heart at this stage because other tissues with L-type Ca^{2+} channels, such as endocrine cells and sensory cells, have yet to develop (Catterall et al., 2005). The dorsal aortae appear normal and facilitate normal blood circulation prior to administration of Nifedipine. This treatment abrogated the pulsing flow in the connected dorsal aortae and led to a scattered distribution of FN fibrils in the adjacent somite-endoderm gap (n=6, right panels in Fig. 5D). Arrest of the heart beating by Nifedipine treatment shortened the length and varied the distribution angles of the FN fibrils, similar to in Ki8751-treated embryos (Fig. 5F,G).

To confirm by a different approach that blood flow-associated vessel expansion is required for adjacent FN pillar formation, we occluded the dorsal aorta by a photodynamic therapy strategy (Robertson et al., 2009). Photo-activation of Visudyne causes blood cells to coagulate and induces local occlusion of blood vessels in the chicken embryo (Debefve et al., 2008). Using this strategy, blood clots were induced anterior to the desired somite levels (SIV) one side of the dorsal aorta (n=5, Fig. 5C) on the left side of the embryo,

Development (2017) 144, 281-291 doi:10.1242/dev.141259

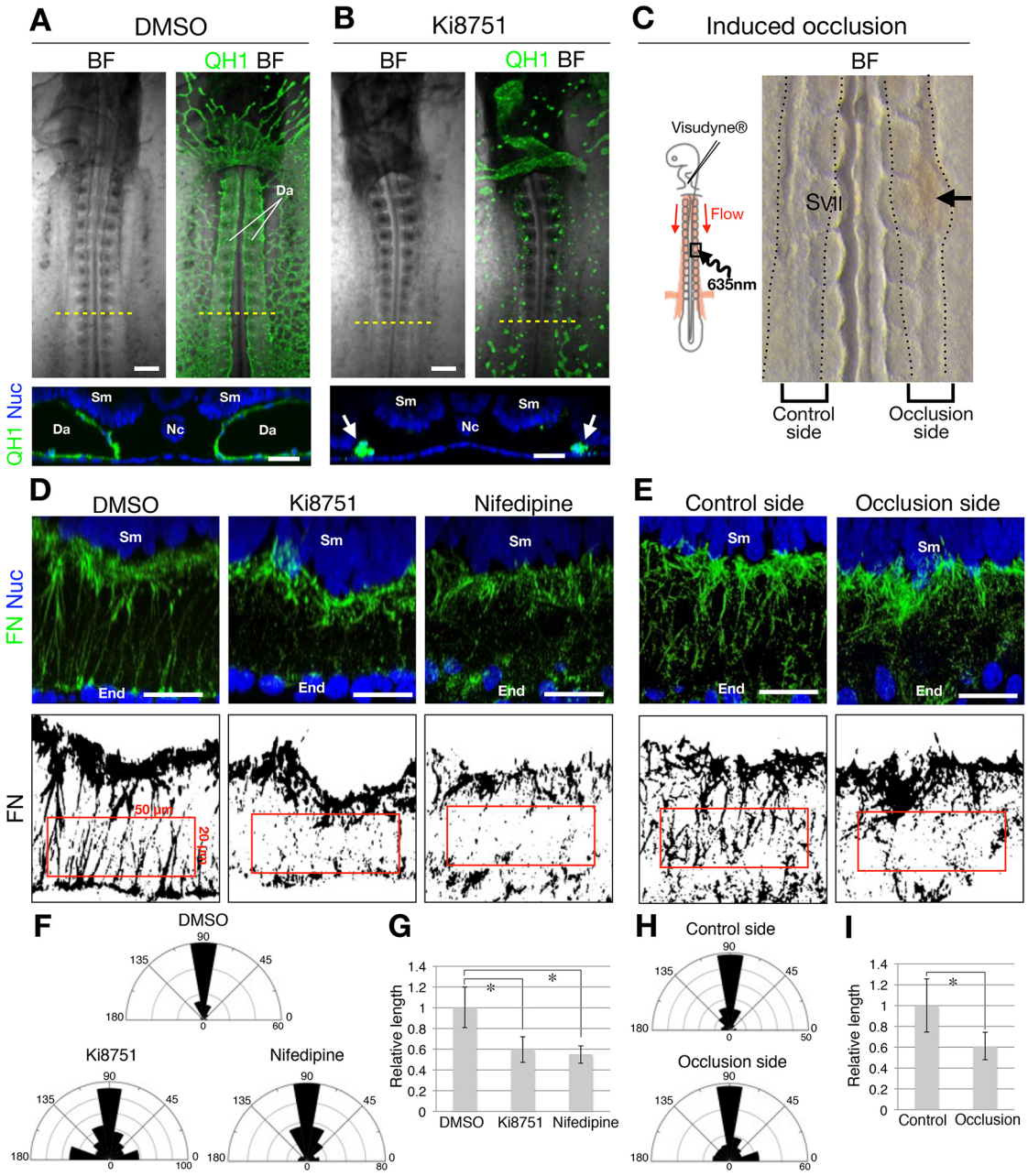

Fig. 5. Blood flow in the dorsal aorta is required for the distribution of FN pillars in the somite-endoderm gap. (A,B) Upper panels show frontal views of a HH stage 12 quail embryo 9 h after administration of control DMSO (A) or Ki8751 (B). Anterior is top. Lower panels show optical transverse sections at the yellow dashed lines. (A) Endothelial cells (ECs) were detected by QH1 immunostaining. QH1^{+} dorsal aorta formed along the longitudinal axis (upper panels) between somites and endoderm (lower panel). (B) Ki8751 treatment disturbed the continuous dorsal aorta formation along the anteroposterior axis (upper panels). ECs did not form luminal structures (arrows in lower panel). The beating function of the heart was intact and the number of somites was not altered (see also Movie 6). (C) Diagram showing the unilateral induction of occlusion in a dorsal aorta (left). Visudyne was injected into the heart at HH stage 13; subsequently, dorsal aorta at the SVII level was exposed to a 635 nm laser. Frontal view of an occlusion-induced embryo 1 h after laser exposure (right panel). Blood clot is indicated by the arrow. (D,E) Longitudinal oblique sections of the ventral part of somites at SIV levels. Upper panels show FN distribution in the somite-endoderm gaps. Lower panels are binary images of FN for quantification. Quantified areas are marked by red boxes. Anterior is left. (F,H) Angle distribution of FN fibrils in a representative embryo for each experiment. Number of FN signals and degrees are indicated in the *r* and θ axes, respectively. (G,I) Lengths of FN fibrils were significantly decreased in Ki8751-treated or Nifedipine-treated embryos, and on the occlusion side. Averages of 377 (DMSO), 763 (Ki8751), 830 (Nifedipine), 333 (control side) and 428 (occlusion side) of FN fibrils in three independent embryos for each condition. *P<0.001 by Student's *t*-test. Error bars represent s.d. Sm, somite; End, endoderm; Da, dorsal aorta; Nc, notochord. Scale bars: 200 µm in upper panels of A,B; 40 µm in lower panels of A,B; 20 µm in D,E.

while the right side served as an unaltered control. After 1 h, the distribution patterns of FN fibrils were compared between control and Visudyne occluded sides. FN fibrils were not organized as pillars on the occluded side (right panels in Fig. 5E). FN pillars were partially disconnected on the control side due to *ex ovo* culture (left panels in Fig. 5E). However, quantification analysis indicates significant angle diversification and shortening of FN fibrils on the occluded side (Fig. 5H,I). Because heart arrest by Nifedipine and dorsal aorta occlusion by Visudyne were performed after establishment of the FN pillars, our data indicate that blood

Development (2017) 144, 281-291 doi:10.1242/dev.141259

flow-associated pulsatile expansion of dorsal aortae is required for the maintenance of adjacent FN pillars.

Basal filopodia are required for somitic cell polarization

We have shown that long filopodia protruding from somitic epithelial cells are aligned and oriented with the FN pillars (Fig. 1). To determine if filopodia play a role in somite morphogenesis, we analyzed the cell-autonomous function of the filopodia by depletion of Ena/VASP (Bear et al., 2000). Early stage somites from SI to VI are characterized by apically gathered pseudostratified epithelium and basally polarized nuclei (Martins et al., 2009). In order to observe how filopodial disruption affects cell shape and nuclear position, we electroporated plasmids expressing H2B-EGFP-2A-FP4-mito or H2B-EGFP-2A-AP4-mito (control) into somitic cells and then tracked the H2B-EGFP$^+$ nuclei, the majority of which are located on the basal side of the somitic epithelial cells. Positions of nuclei and the actin cytoskeleton were fluorescently visualized with H2B-EGFP and co-electroporated LifeAct-mRFPruby, respectively. When a small percentage (10-20%) of the somite cells were electroporated, the control AP4-mito-overexpressing cells adopted apicobasally elongated epithelial shapes and H2B-EGFP$^+$ nuclei that were localized closer to the basal than apical side of the epithelium (n=13, arrows in Fig. 6A). The FP4-mito-overexpressing cells adopted apicobasally elongated epithelial shapes similar to the control cells, indicating that FP4-mito does not perturb epithelial morphology. However, the H2B-EGFP$^+$ nuclei of FP4-mito cells localized more apically than those of AP4-mito cells (n=12, arrows in Fig. 6B).

To dynamically study how filopodia determine nuclear localization in the somitic epithelium, we performed time-lapse imaging analysis of H2B-EGFP-2A-FP4-mito-electroporated somitic cells in PGK:H2B-mCherry transgenic quail embryos (Huss et al., 2015). In somite cells expressing control plasmid (H2B-EGFP-2A-AP4-mito), H2B-EGFP$^+$/H2B-mCherry$^+$ nuclei localized closer to the basal side of the somite epithelium, as was seen for non-electroporated cells (mCherry$^+$, n=5, Fig. 6C, Movie 7). By contrast, the nuclei of somite cells expressing H2B-EGFP-2A-FP4-mito were localized more apically than those of non-electroporated cells (n=5, Fig. 6D, Movie 8). Tracking analysis of H2B-EGFP$^+$ cells revealed that the nuclei of the somite epithelial cells tended to move medioventrally in the control embryo (left panel in Fig. 6E). By contrast, the filopodia-disrupted cell nuclei lost the ability to move medioventrally (right panel in Fig. 6E). The distances moved by nuclei (their track length) were not reduced in the FP4-mito-electroporated cells but there was a significant reduction in their displacement lengths, indicating that the directionality of nuclear migration is perturbed by filopodia disruption (Fig. 6F).

Effect of loss of filopodia on the morphology and differentiation of somites

The medioventral region of the somite differentiates into sclerotome starting at SIV in avian embryos (Christ and Ordahl, 1995). We found that when a high percentage (>40%) of somitic cells was electroporated with FP4-mito, some of their nuclei were found at the basalmost side where the basement membrane marker laminin accumulates (n=15, arrows in Fig. 6G). Somites containing a high population of FP4-mito-electroprated cells seemed to be defective in medioventral expansion compared with control somites. To evaluate this effect of filopodia inhibition on somite morphology quantitatively, we developed an automatic detection and measurement program for the gap spaces in the midline (Fig. S7). We used this program to measure the sizes of the gap spaces (red areas in Fig. 6H) at SIV to X levels in embryos with a high percentage of electroporated somitic cells. The SIV to X level somites in the AP4-mito-electroporated control embryos expanded medioventrally and the gap spaces decreased in size with increasing somite levels (left panels in Fig. 6H and blue line in Fig. 6I). Gap sizes in the FP4-mito-electroporated embryos were larger than in the control embryos throughout the SIV to X levels (right panels in Fig. 6H and red line in Fig. 6I).

To examine whether filopodial disruption influences sclerotome differentiation, total RNA was isolated from SI to VIII level somites within EGFP-AP4-mito-electroporated and EGFP-FP4-mito-electroporated embryos. qRT-PCR was used to quantify the expression levels of the sclerotome differentiation markers *Pax1*, *Ptc1* and *Gli1* (Borycki et al., 2000; Johnson et al., 1994; Marigo and Tabin, 1996). *Pax1*, *Ptc1* and *Gli1* mRNA levels were dramatically reduced in FP4-mito-electroporated compared with AP4-mito-electroporated somites (Fig. 7A). Thus, the defects in sclerotome differentiation seen in embryos with disrupted filopodia correlate with a defect in the medioventral expansion of the somite epithelium at the molecular and cellular levels.

It is known that sclerotome differentiation is induced by Sonic hedgehog (Shh) signaling (Borycki et al., 2000). To assess the possible involvement of the filopodia in Shh transport to the somites, we confirmed the distribution of Shh and its receptor Smoothened (Smo) (Briscoe and Thérond, 2013) in normal quail embryos by immunostaining. Shh was detected around the tips of the filopodia in the somite-endoderm gap. Smo was also found along the filopodia (Fig. 7B,C). These results suggest that the basal filopodia might also be used to transport Shh protein and thus signals from endoderm and/or notochord to the somites.

DISCUSSION

This study demonstrates a novel type of FN distribution pattern: FN fibrils are patterned as pillars along extended lines of the longitudinal axes of somitic epithelial cells (Fig. 1). We have addressed how the FN pillars are established in the somite-endoderm gap and suggest new mechanisms underlying specialized FN distribution: (1) long filopodia protruding from the basal surface of the somite epithelium extend along the FN pillars and reach the endoderm; (2) these filopodia regulate FN assembly through α5β1-integrins and talin; (3) mechanical force propagated from pulsating dorsal aorta maintains the unidirectional alignment of the FN pillars; (4) the filopodia direct migration of the somite epithelial cell nuclei towards the basal edge and regulate somite morphogenesis. These findings suggest that pulsations of the dorsal aorta interact with the mechanical properties of FN (e.g. unfolding, polymerization and stretching) to establish the FN pillars that bridge the somite-endoderm gap (Fig. 7D).

Spatiomechanical organization of FN pillars in the somite-endoderm gap

It has previously been reported that dorsal epithelial cells in the somites protrude filopodia toward ectoderm during segmentation (S0 level; Martins et al., 2009) and myotome differentiation (SVIII level; Sagar et al., 2015). Our study demonstrates that ventral somite epithelial cells protrude filopodia toward endoderm (S0 to VI levels, Fig. 1, Fig. S1). Therefore, filopodia protrude from the somite epithelial cells regardless of whether dorsal or ventral side. In both cases, the filopodia might help fasten the somites to surrounding tissue layers through elaboration of FN fibrils and other ECM components.

The somitic filopodia exhibit vibrant elongation/retraction movements (Fig. 1, Movie 1) that resemble the well-known dynamic behaviors of filopodia observed *in vitro*. Normal functioning of the

Development (2017) 144, 281-291 doi:10.1242/dev.141259

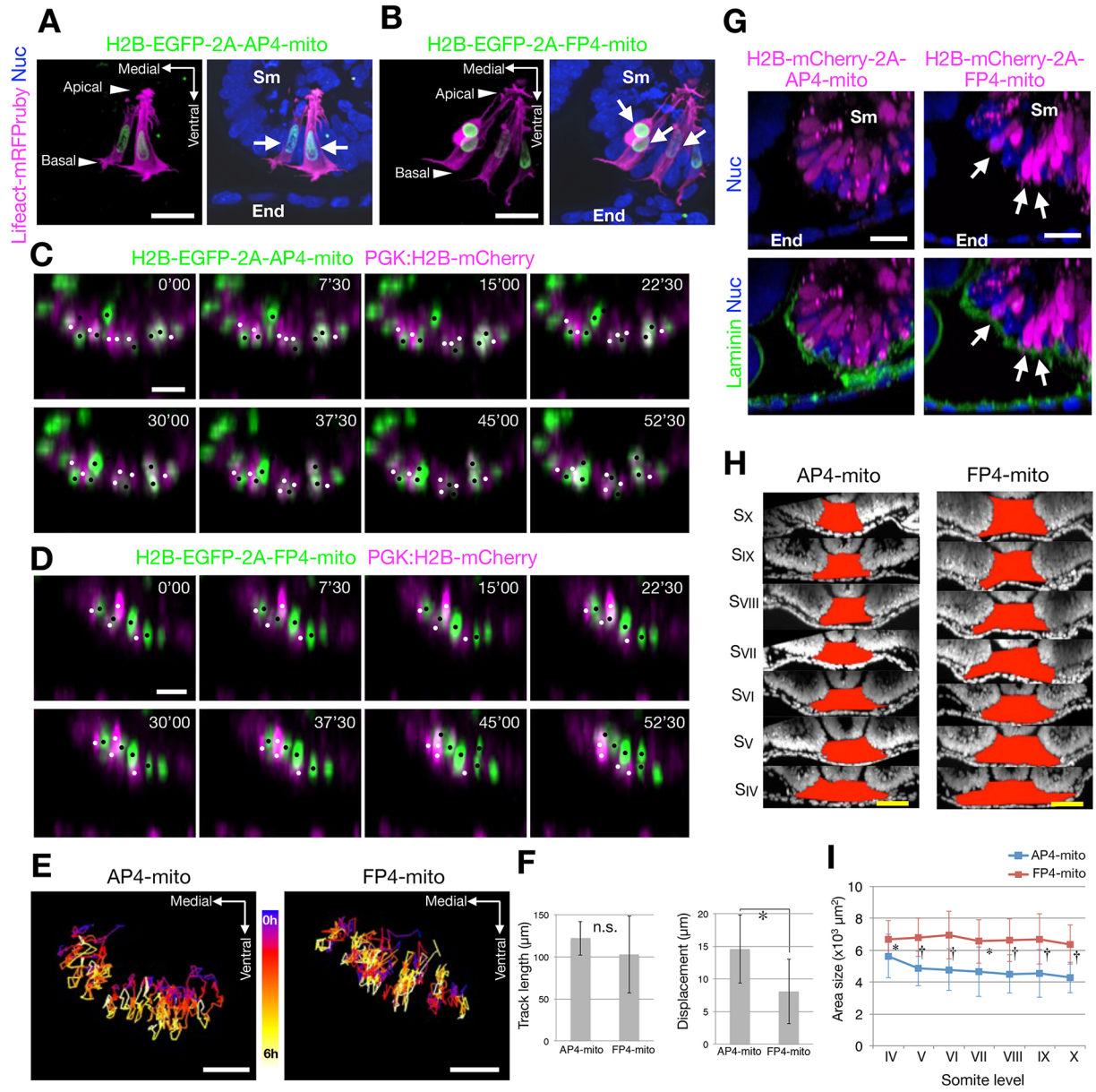

Fig. 6. Disruption of filopodia in the somites affects somite morphogenesis. (A,B) Optical transverse sections at SIV levels of H2B-EGFP-2A-AP4-mito- and H2B-EGFP-2A-FP4-mito-electroporated embryos at HH stage 12. AP4-mito- and FP4-mito-overexpressing cells were detected using EGFP in nuclei and cell shape was visualized by LifeAct-mRFPruby. AP4-mito-expressing cells elongated along the apicobasal axis. EGFP$^+$ nuclei were located in the basal side (A). EGFP$^+$ nuclei were located at the middle level of the epithelial column in the FP4-mito-electroporated somite (arrows in B). (C,D) Time-lapse imaging of filopodia-disrupted somitic cells in PGK:H2B-mCherry transgenic quail embryos. A time series is shown of optical transverse sections during the SII to VI transition in HH stage 12 embryos. See also Movies 7 and 8. In a control somite, EGFP$^+$ AP4-mito-overexpressing cell nuclei (black dots in C) are found in the basalmost side of the epithelium, as in non-electroporated cells (white dots in C). In a FP4-mito-overexpressing somite, EGFP$^+$ nuclei (black dots in D) were not located in the basalmost side, whereas non-electroporated cell nuclei (white dots in D) are preferentially observed in the basalmost position. (E) Trajectories of EGFP signals during SII to VI transition in the AP4-mito- and FP4-mito-overexpressing somites. (F) Track length and displacement of the AP4-mito- and FP4-mito-expressing cells were compared. Averages of 63 (AP4-mito) and 72 (FP4-mito) tracks in three independent embryos for each condition. *P<0.001 by Student's t-test. Error bars represent s.d. (G) Optical transverse sections at SVI levels of H2B-mCherry-2A-AP4-mito- and H2B-mCherry-2A-FP4-mito-electroporated embryos at HH stage 12. Laminin indicates basement membrane (lower panels). FP4-mito-overexpressing cell nuclei (mCherry$^+$) were found at the basal side next to the laminin (arrows). (H) Detection and measurement of the gap spaces framed by somites, endoderm and neural tube by the DP approach (Bellman and Dreyfus, 1962). Details are described in Fig. S6. The gaps (filled with red) in a FP4-mito-electroporated embryo (right) were larger than those in an AP4-mito electroporated embryo (left). (I) Average size of the gaps in AP4-mito-overexpressing (n=15) and FP4-mito-overexpressing (n=16) embryos at each somite level. Error bars represent s.d. *P<0.01, †P<0.001 by Student's t-test. Scale bars: 20 μm in A-E,G; 50 μm in H.

filopodia is crucial to the formation of the FN pillars. We showed that disruption of the filopodia caused the FN pillars to disappear (Fig. 2). We propose that the dynamic protrusive activity of the filopodia might help to rearrange the pre-existing FN fibrils into pillars, possibly fine-tuning interactions between tissues that are elongating and expanding at different rates during embryo growth (Huss et al., 2015). The heart beat-driven pulsations of the dorsal aortae also appear to help establish, pattern and/or stabilize the FN pillars. When formation of the dorsal aortae was disrupted or blood flow through them was disturbed, the adjacent pillars were disrupted (the FN fibrils became scattered but did

Development (2017) 144, 281-291 doi:10.1242/dev.141259

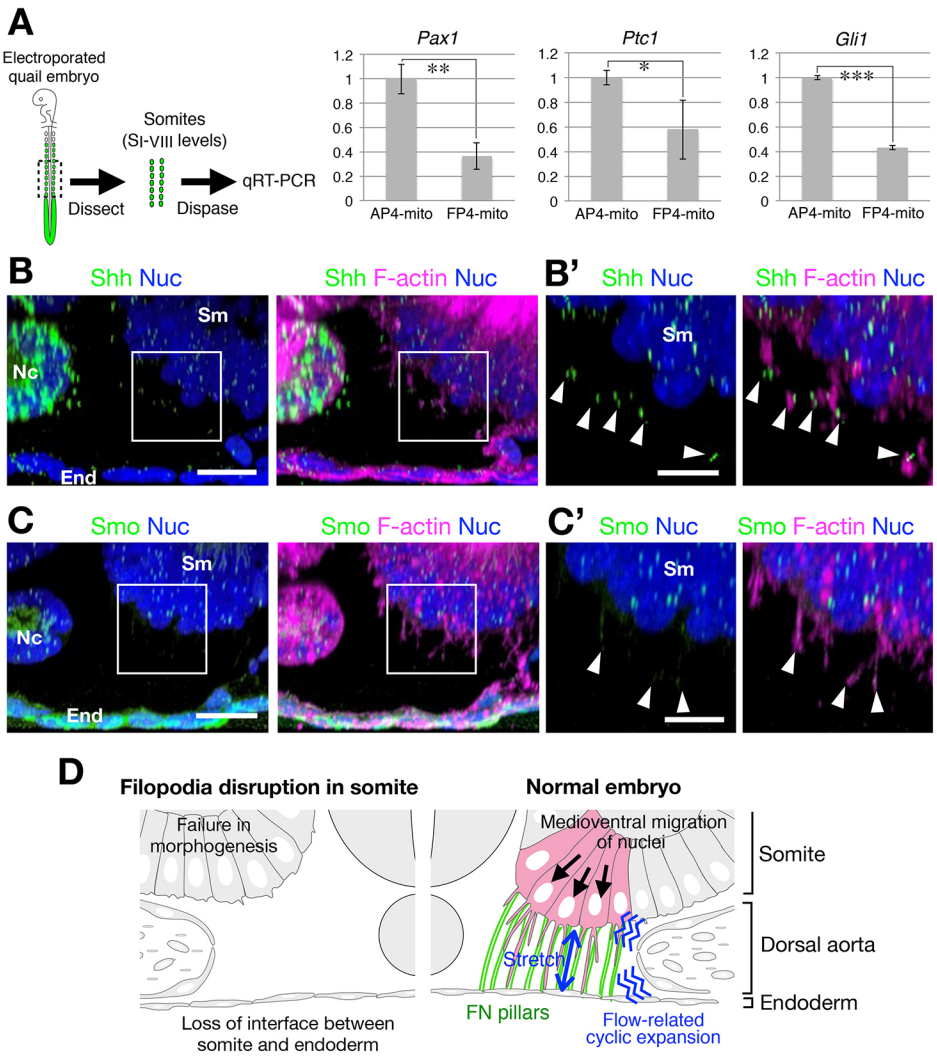

Fig. 7. Implication of basal filopodia involvement in Shh signaling and a model depicting how the somite-endoderm gap space is mechanically supported. (A) Comparison of expression levels of somite differentiation marker genes in EGFP-AP4-mito- and EGFP-FP4-mito-electroporated somites. Total RNA was collected from somites at SI to VIII levels of four embryos and subjected to qRT-PCR. Relative expression levels of *Pax1*, *Ptc1* and *Gli1* were decreased in the FP4-mito-overexpressing somites. **P*<0.05, ***P*<0.01, ****P*<0.001 by Student's *t*-test. Error bars represent s.d. (B-C′) Optical transverse sections at SIV levels in HH stage 12 embryos. Boxed regions are magnified in B′ and C′. (B) Shh was detected in notochord, endoderm, somite and around the tips of the filopodia as indicated by F-actin-rich spikes (arrowheads in B′). (C) Smo was detected in the notochord, endoderm, somite and along the filopodia (arrowheads in C′). Sm, somite; End, endoderm; Nc, notochord. (D) Basal filopodia in the somite epithelial cells function in FN pillar formation cooperatively with cyclic expansion of the adjacent dorsal aorta, and this would make the somite-endoderm gap stretchable. Scale bars: 20 µm in B,C; 10 µm in B′,C′.

not disappear; Fig. 5). This difference suggests that filopodia and vascular pulsation stress regulate FN pillar formation by distinct processes: the filopodia act predominantly to exert the cellular force required for the initial assembly and unfolding of FN, while vascular pulsation forces provide unidirectional stretch that maintains the polymerized state of FN.

Role of basal filopodia in somite morphogenesis

The nuclei of somitic cells, like those of most cells in pseudostratified epithelia, lie closer to the basal ends of the cells. In FP4-mito-overexpressing cells this polarization was disrupted: their nuclei localized closer to the center of the cell than those of AP4-mito-overexpressing cells (Fig. 6B,D). This suggests that filopodial contacts with FN pillars might help to localize the nuclei of somite cells toward the basal end. It has been reported that unidirectional cyclic stretching orients actin stress fibers along the stretch axis, and cells are subsequently aligned parallel to the force (Hoffman et al., 2011). We hypothesize that pulsatile force arising from the dorsal aorta is transmitted to force-sensing adapter proteins at the filopodium and leads to cytoskeletal reorganization. Nesprin is known to connect the F-actin cytoskeleton and nucleus along the direction of cell-ECM mechanical force (Wang et al., 2009). The polarized nuclear migration that we observed in the somite epithelium might be regulated by such force propagation mechanisms between the ECM and nuclei.

Moreover, we found that when a large percentage of somitic cells had their filopodia disrupted by FP4-mito overexpression, medioventral expansion of the somites was blocked (Fig. 6G,H). Disruption of the FN pillars by overexpression of 70 kDa qFN or *FN1* shRNA caused defects similar to those observed in the FP4-mito-electroporated embryos (Fig. S5), suggesting that FN pillars collaborate with filopodia in the medioventral expansion of the somites. We would expect that larger numbers of FP4-mito-overexpressing cells are more likely to disrupt FN pillars (Fig. 2), resulting in loss of FN interfaces between the somites and endoderm.

Intriguingly, Ena/VASP are enriched in somite boundaries and their depletion by FP4-mito overexpression causes failure of somitic cell rotation and FN distribution in *Xenopus* embryos (Kragtorp and Miller, 2006), suggesting a conserved role of Ena/VASP proteins in somitogenesis between non-amniotes and amniotes. However, it is likely that blood flow-associated mechanical forces are not initiated in these non-amniote embryos at early somitogenesis because dorsal aortae are observed as clusters of ECs without lumen (Cleaver and Krieg, 1998; Jin et al., 2005). Consistently, the long axes of FN fibrils are oriented according to planar cell polarity in non-amniotes (Davidson et al., 2006; Latimer and Jessen, 2010). The large acellular space between the somites and endoderm observed in amniote embryos is thought to have arisen in association with earlier lumenization and functioning of the dorsal aorta. As it has been shown that fibrillar FN has elastic properties (Little et al., 2008;

Development (2017) 144, 281-291 doi:10.1242/dev.141259

Smith et al., 2007), the FN pillars are expected to provide a stretchable space that allows the dorsal aorta to cyclically pulsate.

Potential involvement of the basal filopodia in morphogen signaling in the somites

Actin-based cellular protrusions called cytonemes protrude from some cells. The cytonemes have been shown to make signaling proteins and extend to cells with receptors for those proteins. For example, cytonemes help mediate Hedgehog signaling in fly (Bischoff et al., 2013; Kornberg and Roy, 2014). Similarly, in vertebrate embryos, long filopodia convey Shh in the developing limb bud and Wnt in the dorsal side of somites (Sanders et al., 2013; Sagar et al., 2015). We demonstrated the localization of Shh and Smo around filopodia in somite epithelial cells and provide supporting data for the requirement of filopodia for activation of the Shh signaling pathway (Fig. 7). Further studies are needed to clarify whether filopodia also transport Shh signals from nearby endoderm and/or notochord tissues to the somites.

MATERIALS AND METHODS

Ethics statement

All experimental methods and animal husbandry procedures were performed in accordance with the guidelines of the Federation of European Laboratory Animal Science Associations and with the approval of the Institutional Animal Care and Use Committees at Kumamoto University and Kyushu University.

Quail embryos

Wild-type Japanese quails (*Coturnix c. japonica*) were provided by Dr Tamao Ono (Shinsyu University, Japan) and Tokai-yuki (Aichi, Japan). The PGK:H2B-mCherry transgenic quail (Huss et al., 2015) was obtained from the Department of Animal Resource, University of Southern California (USA). Quail strains were bred at Animal Resources and Development, Kumamoto University (Japan) and the quail breeding facility at Kyushu University (Japan) according to Huss et al. (2008). Fertilized quail eggs were incubated at 37°C until electroporation (supplementary Materials and Methods) and subsequent analysis. Staging of quail embryos was based on the Hamburger and Hamilton (HH) stages of chicken embryos (Hamburger and Hamilton, 1951).

Ki8751 and Nifedipine treatments

Ki8751 (Santa Cruz Biotechnology) stock solution (10 mM in DMSO) was diluted with Hanks' Balanced Salt solution (HBSS) to 0.2 mM. Then, 250 µl of 0.2 mM Ki8751 was injected into the yolk at the 10-somite stage *in ovo* and incubated for 9 h until fixation. Because the total volume of the quail egg is ∼5 ml, the final concentration of Ki8751 *in ovo* was 10 µM. Nifedipine (Nakalai) stock solution (100 mM in water) was diluted with HBSS to 100 µM. Then, 500 µl of 100 µM Nifedipine was administered to the embryos at the 16-somite stage *in ovo* and incubated for 1 h at 37°C until fixation. The final concentration of Nifedipine *in ovo* was 10 µM.

Induction of dorsal aorta occlusion

Quail embryos were developed *in ovo* until HH stage 13 and then transferred *ex ovo* as described (Chapman et al., 2001). The embryos were placed ventral side up on agar-albumen medium. Visudyne (Novartis Pharma) was diluted with HBSS to 2 µM and 10 µl was injected into the heart tube using a glass capillary and incubated for 10 min at 37°C to circulate the Visudyne. Upstream levels of the dorsal aorta demarcated as regions of interest (ROIs) were exposed to a 635 nm full-power laser for 1 min using the photo-stimulation program of a Fluoview 1200 (Olympus). Embryos were incubated for 1 h at 37.0°C until fixation.

Molecular biology

Quail cDNA cloning and plasmid constructions are described, with associated RT-PCR primers and universal linker sets or hairpin sequences, in the supplementary Materials and Methods. Knockdown efficiency of the shRNA constructs was assessed in transfected quail embryonic fibroblasts by qPCR as described in the supplementary Materials and Methods.

Immunostaining and *in situ* hybridization

Antibodies for immunostaining and digoxigenin-labeled antisense RNA probes for *in situ* hybridization are described in the supplementary Materials and Methods. Confocal microscopy of immunostained embryos, including the measurement of FN fibrils in 3D reconstructed images, was performed as described in the supplementary Materials and Methods.

Time-lapse microscopy

Electroporated quail embryos were developed *in ovo* until HH stage 12, transferred to *ex ovo* and subjected to time-lapse confocal imaging and image analysis with Imaris (Bitplane) as described in the supplementary Materials and Methods.

Measurement of gap space size

EGFP-AP4-mito-electroporated and EGFP-FP4-mito-electroporated quail embryos at HH stage 12 were fixed and nuclei stained with Hoechst. 3D reconstructed images were optically transversely sectioned at the mid-levels of each somite and the images binarized. Approximate gap space size was then measured as described in detail in the supplementary Materials and Methods.

Acknowledgements

We thank Dr Frank Gertler (MIT) for kindly providing EGFP-AP4-mito and EGFP-FP4-mito; Dr Takaya Abe (RIKEN, CLST) and Dr Shinichi Aizawa (RIKEN, CDB) for the kind gift of Lyn-mCherry; Dr Tamao Ono (Shinshu University) for wild-type Japanese quails; Dr Kenji Shimamura (Kumamoto University), Dr Takayuki Suzuki (Nagoya University), Dr Takashi Miura (Kyushu University) and Dr Tadashi Nomura (Kyoto Prefectural University of Medicine) for helpful discussions; Dr Gabrielle G. Leblanc for critical reading of the manuscript; the Program of the Joint Usage Research Center for Developmental Medicine, Institute of Molecular Embryology and Genetics, Kumamoto University; and the Research Center for Human Disease Modeling, Kyushu University.

Competing interests

The authors declare no competing or financial interests.

Author contributions

Y.S. designed and performed experiments, and analyzed data. Y.S. and R.L. wrote the manuscript. K.N. and Y.I. constructed expression vectors. A.H. and S.U. performed quantification of images. D.H. and R.L. generated the PGK:H2B-mCherry transgenic quail line and LifeAct vectors.

Funding

This work was supported by grants from the Japan Society for the Promotion of Science KAKENHI (23111523, 24770215), Japan Science and Technology Agency PRESTO, Takeda Science Foundation and Sumitomo Foundation to Y.S.

Supplementary information

Supplementary information available online at
http://dev.biologists.org/lookup/doi/10.1242/dev.141259.supplemental

References

Abe, T., Kiyonari, H., Shioi, G., Inoue, K.-I., Nakao, K., Aizawa, S. and Fujimori, T. (2011). Establishment of conditional reporter mouse lines at ROSA26 locus for live cell imaging. *Genesis* **49**, 579-590.

Argraves, W. S., Larue, A. C., Fleming, P. A. and Drake, C. J. (2002). VEGF signaling is required for the assembly but not the maintenance of embryonic blood vessels. *Dev. Dyn.* **225**, 298-304.

Baneyx, G., Baugh, L. and Vogel, V. (2001). Coexisting conformations of fibronectin in cell culture imaged using fluorescence resonance energy transfer. *Proc. Natl. Acad. Sci. USA* **98**, 14464-14468.

Baneyx, G., Baugh, L. and Vogel, V. (2002). Fibronectin extension and unfolding within cell matrix fibrils controlled by cytoskeletal tension. *Proc. Natl. Acad. Sci. USA* **99**, 5139-5143.

Bear, J. E. and Gertler, F. B. (2009). Ena/VASP: towards resolving a pointed controversy at the barbed end. *J. Cell Sci.* **122**, 1947-1953.

Bear, J. E., Loureiro, J. J., Libova, I., Fässler, R., Wehland, J. and Gertler, F. B. (2000). Negative regulation of fibroblast motility by Ena/VASP proteins. *Cell* **101**, 717-728.

Bellman, R. and Dreyfus, S. E. (1962). *Applied Dynamic Programming*. Princeton, NJ: Princeton University Press.
Bischoff, M., Gradilla, A.-C., Seijo, I., Andrés, G., Rodríguez-Navas, C., González-Méndez, L. and Guerrero, I. (2013). Cytonemes are required for the establishment of a normal Hedgehog morphogen gradient in Drosophila epithelia. *Nat. Cell Biol.* **15**, 1269-1281.
Bkaily, G., El-Bizri, N., Bui, M., Sukarieh, R., Jacques, D. and Fu, M. L. X. (2003). Modulation of intracellular Ca2+ via L-type calcium channels in heart cells by the autoantibody directed against the second extracellular loop of the alpha1-adrenoceptors. *Can. J. Physiol. Pharmacol.* **81**, 234-246.
Borycki, A., Brown, A. M. and Emerson, C. P., Jr. (2000). Shh and Wnt signaling pathways converge to control Gli gene activation in avian somites. *Development* **127**, 2075-2087.
Bower, D. V., Sato, Y. and Lansford, R. (2011). Dynamic lineage analysis of embryonic morphogenesis using transgenic quail and 4D multispectral imaging. *Genesis* **49**, 619-643.
Briscoe, J. and Thérond, P. P. (2013). The mechanisms of Hedgehog signalling and its roles in development and disease. *Nat. Rev. Mol. Cell Biol.* **14**, 418-431.
Catterall, W. A., Perez-Reyes, E., Snutch, T. P. and Striessnig, J. (2005). International Union of Pharmacology. XLVIII. Nomenclature and structure-function relationships of voltage-gated calcium channels. *Pharmacol. Rev.* **57**, 411-425.
Chapman, S. C., Collignon, J., Schoenwolf, G. C. and Lumsden, A. (2001). Improved method for chick whole-embryo culture using a filter paper carrier. *Dev. Dyn.* **220**, 284-289.
Christ, B. and Ordahl, C. P. (1995). Early stages of chick somite development. *Anat. Embryol.* **191**, 381-396.
Cleaver, O. and Krieg, P. A. (1998). VEGF mediates angioblast migration during development of the dorsal aorta in Xenopus. *Development* **125**, 3905-3914.
Das, R. M., Van Hateren, N. J., Howell, G. R., Farrell, E. R., Bangs, F. K., Porteous, V. C., Manning, E. M., McGrew, M. J., Ohyama, K., Sacco, M. A. et al. (2006). A robust system for RNA interference in the chicken using a modified microRNA operon. *Dev. Biol.* **294**, 554-563.
Davidson, L. A., Marsden, M., Keller, R. and DeSimone, D. W. (2006). Integrin alpha5beta1 and fibronectin regulate polarized cell protrusions required for Xenopus convergence and extension. *Curr. Biol.* **16**, 833-844.
Debefve, E., Pegaz, B., van den Bergh, H., Wagnières, G., Lange, N. and Ballini, J.-P. (2008). Video monitoring of neovessel occlusion induced by photodynamic therapy with verteporfin (Visudyne), in the CAM model. *Angiogenesis* **11**, 235-243.
DuFort, C. C., Paszek, M. J. and Weaver, V. M. (2011). Balancing forces: architectural control of mechanotransduction. *Nat. Rev. Mol. Cell Biol.* **12**, 308-319.
Dzamba, B. J., Jakab, K. R., Marsden, M., Schwartz, M. A. and DeSimone, D. W. (2009). Cadherin adhesion, tissue tension, and noncanonical Wnt signaling regulate fibronectin matrix organization. *Dev. Cell* **16**, 421-432.
Girós, A., Grgur, K., Gossler, A. and Costell, M. (2011). alpha5beta1 integrin-mediated adhesion to fibronectin is required for axis elongation and somitogenesis in mice. *PLoS ONE* **6**, e22002.
Gomes de Almeida, P. G., Pinheiro, G. G., Nunes, A. M., Goncalves, A. B. and Thorsteinsdottir, S. (2016). Fibronectin assembly during early embryo development: a versatile communication system between cells and tissues. *Dev. Dyn.* **245**, 520-535.
Hamburger, V. and Hamilton, H. L. (1951). A series of normal stages in the development of the chick embryo. *J. Morphol.* **88**, 49-92.
Hoffman, B. D., Grashoff, C. and Schwartz, M. A. (2011). Dynamic molecular processes mediate cellular mechanotransduction. *Nature* **475**, 316-323.
Hoffmann, C., Leroy-Dudal, J., Patel, S., Gallet, O. and Pauthe, E. (2008). Fluorescein isothiocyanate-labeled human plasma fibronectin in extracellular matrix remodeling. *Anal. Biochem.* **372**, 62-71.
Huss, D., Poynter, G. and Lansford, R. (2008). Japanese quail (Coturnix japonica) as a laboratory animal model. *Lab. Anim. (NY)* **37**, 513-519.
Huss, D., Benazeraf, B., Wallingford, A., Filla, M., Yang, J., Fraser, S. E. and Lansford, R. (2015). A transgenic quail model that enables dynamic imaging of amniote embryogenesis. *Development* **142**, 2850-2859.
Hytönen, V. P. and Wehrle-Haller, B. (2016). Mechanosensing in cell–matrix adhesions–Converting tension into chemical signals. *Exp. Cell Res.* **343**, 35-41.
Jiang, G., Giannone, G., Critchley, D. R., Fukumoto, E. and Sheetz, M. P. (2003). Two-piconewton slip bond between fibronectin and the cytoskeleton depends on talin. *Nature* **424**, 334-337.
Jin, S.-W., Beis, D., Mitchell, T., Chen, J.-N. and Stainier, D. Y. R. (2005). Cellular and molecular analyses of vascular tube and lumen formation in zebrafish. *Development* **132**, 5199-5209.
Johnson, R. L., Laufer, E., Riddle, R. D. and Tabin, C. (1994). Ectopic expression of Sonic hedgehog alters dorsal-ventral patterning of somites. *Cell* **79**, 1165-1173.
Jülich, D., Cobb, G., Melo, A. M., McMillen, P., Lawton, A. K., Mochrie, S. G., Rhoades, E. and Holley, S. A. (2015). Cross-scale integrin regulation organizes ECM and tissue topology. *Dev. Cell* **34**, 33-44.
Kornberg, T. B. and Roy, S. (2014). Cytonemes as specialized signaling filopodia. *Development* **141**, 729-736.
Koshida, S., Kishimoto, Y., Ustumi, H., Shimizu, T., Furutani-Seiki, M., Kondoh, H. and Takada, S. (2005). Integrinalpha5-dependent fibronectin accumulation for maintenance of somite boundaries in zebrafish embryos. *Dev. Cell* **8**, 587-598.
Kragtorp, K. A. and Miller, J. R. (2006). Regulation of somitogenesis by Ena/VASP proteins and FAK during Xenopus development. *Development* **133**, 685-695.
Latimer, A. and Jessen, J. R. (2010). Extracellular matrix assembly and organization during zebrafish gastrulation. *Matrix Biol.* **29**, 89-96.
Little, W. C., Smith, M. L., Ebneter, U. and Vogel, V. (2008). Assay to mechanically tune and optically probe fibrillar fibronectin conformations from fully relaxed to breakage. *Matrix Biol.* **27**, 451-461.
Marigo, V. and Tabin, C. J. (1996). Regulation of patched by sonic hedgehog in the developing neural tube. *Proc. Natl. Acad. Sci. USA* **93**, 9346-9351.
Martins, G. G., Rifes, P., Amândio, R., Rodrigues, G., Palmeirim, I. and Thorsteinsdóttir, S. (2009). Dynamic 3D cell rearrangements guided by a fibronectin matrix underlie somitogenesis. *PLoS ONE* **4**, e7429.
Moser, M., Legate, K. R., Zent, R. and Fassler, R. (2009). The tail of integrins, talin, and kindlins. *Science* **324**, 895-899.
Navedo, M. F. and Santana, L. F. (2013). CaV1.2 sparklets in heart and vascular smooth muscle. *J. Mol. Cell. Cardiol.* **58**, 67-76.
Ordahl, C. (1993). Myogenic lineages within the developing somite. In *Molecular Basis of Morphogenesis* (ed. M. Bernfield), pp. 165-176. New York: John Wiley and Sons.
Pardanaud, L., Altmann, C., Kitos, P., Dieterlen-Lievre, F. and Buck, C. A. (1987). Vasculogenesis in the early quail blastodisc as studied with a monoclonal antibody recognizing endothelial cells. *Development* **100**, 339-349.
Riedl, J., Crevenna, A. H., Kessenbrock, K., Yu, J. H., Neukirchen, D., Bista, M., Bradke, F., Jenne, D., Holak, T. A., Werb, Z. et al. (2008). Lifeact: a versatile marker to visualize F-actin. *Nat. Methods* **5**, 605-607.
Rifes, P. and Thorsteinsdóttir, S. (2012). Extracellular matrix assembly and 3D organization during paraxial mesoderm development in the chick embryo. *Dev. Biol.* **368**, 370-381.
Rifes, P., Carvalho, L., Lopes, C., Andrade, R. P., Rodrigues, G., Palmeirim, I. and Thorsteinsdottir, S. (2007). Redefining the role of ectoderm in somitogenesis: a player in the formation of the fibronectin matrix of presomitic mesoderm. *Development* **134**, 3155-3165.
Robertson, C. A., Evans, D. H. and Abrahamse, H. (2009). Photodynamic therapy (PDT): a short review on cellular mechanisms and cancer research applications for PDT. *J. Photochem. Photobiol. B Biol.* **96**, 1-8.
Rozario, T. and DeSimone, D. W. (2010). The extracellular matrix in development and morphogenesis: a dynamic view. *Dev. Biol.* **341**, 126-140.
Sagar, D., Prols, F., Wiegreffe, C. and Scaal, M. (2015). Communication between distant epithelial cells by filopodia-like protrusions during embryonic development. *Development* **142**, 665-671.
Sanders, T. A., Llagostera, E. and Barna, M. (2013). Specialized filopodia direct long-range transport of SHH during vertebrate tissue patterning. *Nature* **497**, 628-632.
Sato, Y. (2013). Dorsal aorta formation: separate origins, lateral-to-medial migration, and remodeling. *Dev. Growth Differ.* **55**, 113-129.
Shattil, S. J., Kim, C. and Ginsberg, M. H. (2010). The final steps of integrin activation: the end game. *Nat. Rev. Mol. Cell Biol.* **11**, 288-300.
Smith, M. L., Gourdon, D., Little, W. C., Kubow, K. E., Eguiluz, R. A., Luna-Morris, S. and Vogel, V. (2007). Force-induced unfolding of fibronectin in the extracellular matrix of living cells. *PLoS Biol.* **5**, e268.
Wang, N., Tytell, J. D. and Ingber, D. E. (2009). Mechanotransduction at a distance: mechanically coupling the extracellular matrix with the nucleus. *Nat. Rev. Mol. Cell Biol.* **10**, 75-82.
Zhang, X., Jiang, G., Cai, Y., Monkley, S. J., Critchley, D. R. and Sheetz, M. P. (2008). Talin depletion reveals independence of initial cell spreading from integrin activation and traction. *Nat. Cell Biol.* **10**, 1062-1068.
Zhong, C., Chrzanowska-Wodnicka, M., Brown, J., Shaub, A., Belkin, A. M. and Burridge, K. (1998). Rho-mediated contractility exposes a cryptic site in fibronectin and induces fibronectin matrix assembly. *J. Cell Biol.* **141**, 539-551.